Superconducting materials: What we learn from the heavy Fermions

Z. Fisk, UC Irvine

KITP February 10, 2010

Collaborators

H. R. Ott

D. Pines

D. J. Scalapino

J. D. Thompson

Support: NSF-DMR-0801253 and AFOSR MURI

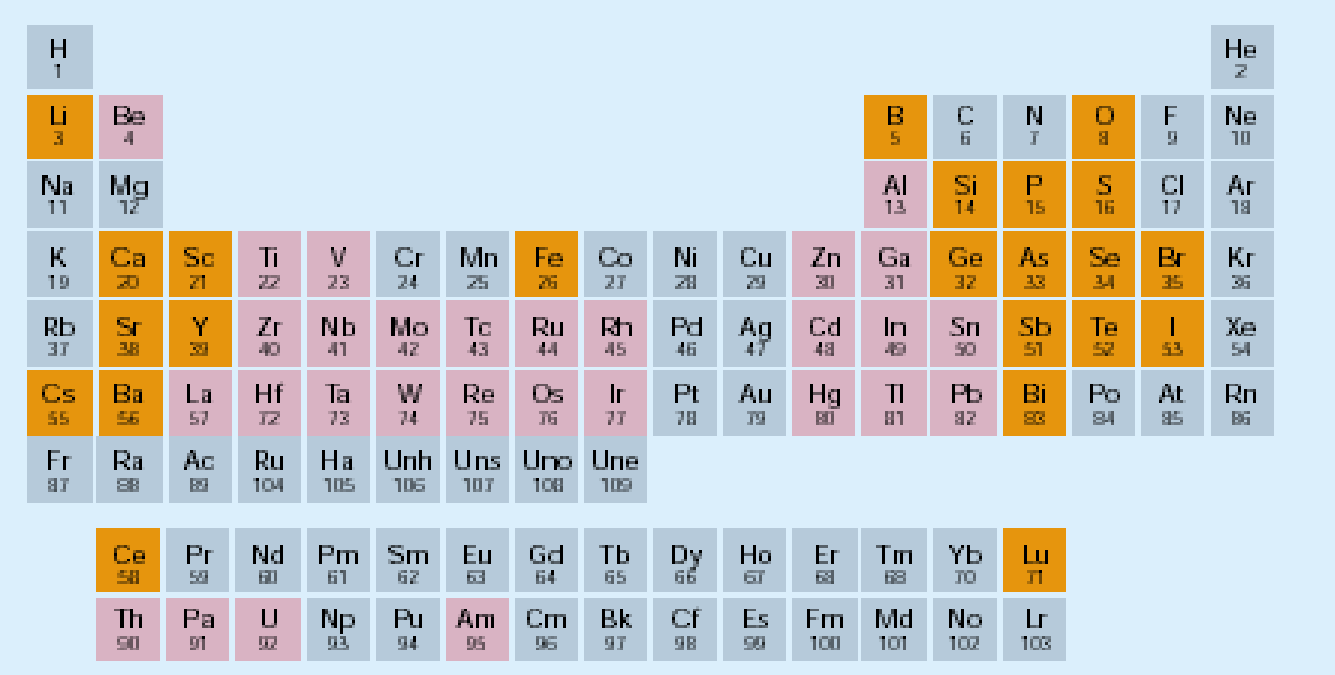

Figure 1 Superconductors under pressure. The colour code of this periodic table (adapted from ref. 13) shows elements that superconduct under normal, atmospheric pressure conditions (purple) and those that superconduct when subjected to high pressure (orange). Shimizu *et al.*[1] confirm the superconductivity of lithium at high pressure, bringing the number of such elements to 23. Under normal pressure conditions, 29 elements are superconductors.

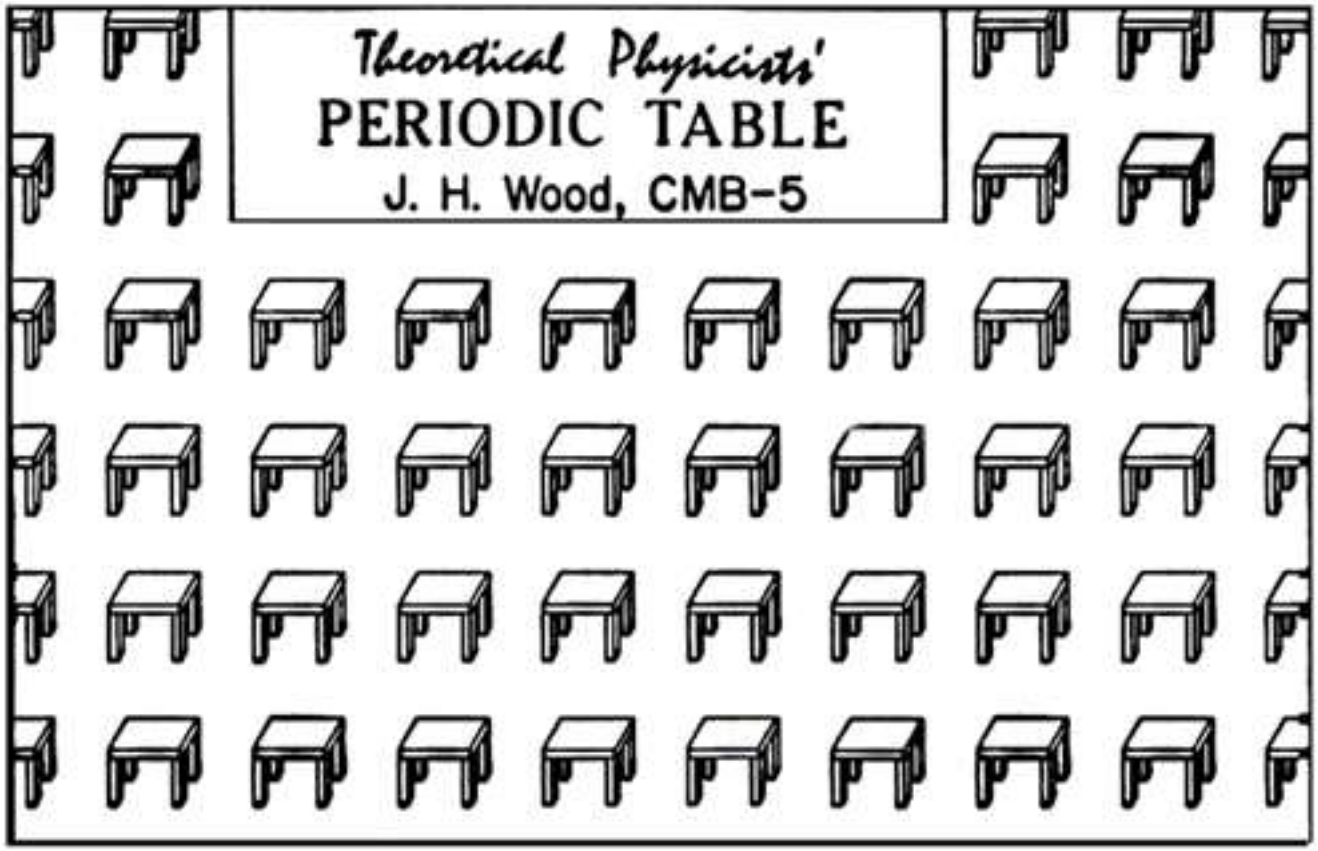
Theoretical Physicists'
PERIODIC TABLE
J. H. Wood, CMB-5

Outline

- generic features of heavy Fermion superconductivity
- similarities in other classes of superconductor
- strong superconductivity
- materials implications

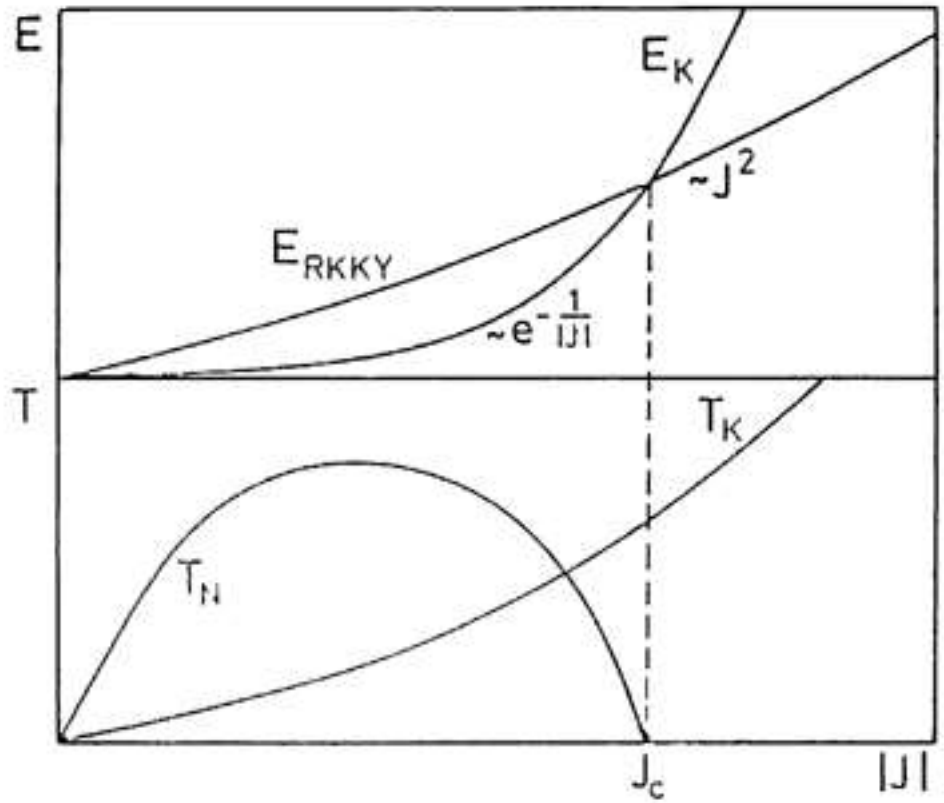

top - Dependences of the characteristic energies connected to the Kondo effect and the RKKY interactions as function of the coupling constant J.
below - Connected "phase diagram".

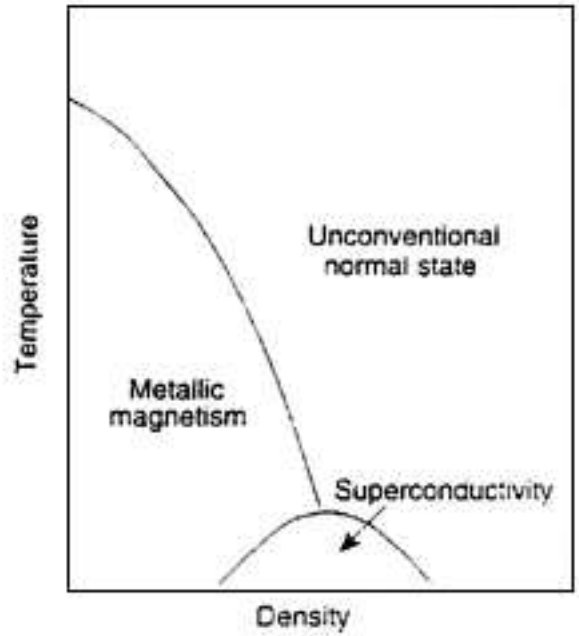

Figure 1 Possible temperature–density phase diagram of a pure metal in which magnetic order is quenched gradually with increasing lattice density. Near the critical density n_c, where the magnetic transition temperature vanishes, magnetic interactions become strong and long-range. The normal state is expected to be anomalous here and, at sufficiently low temperatures, it is expected to give way to a kind of superconductivity in which Cooper pairs are bound together by a glue of magnetic origin. Superconductivity may exist only over a very narrow range of densities near n_c–which is where magnetic interactions overwhelm other channels. Moreover, superconductivity may exist only in samples in which the carrier mean free path exceeds the superconducting coherence length. In most cases this requires samples of very high purity.

Mathur et al. Nature **394**, 39 (1998)

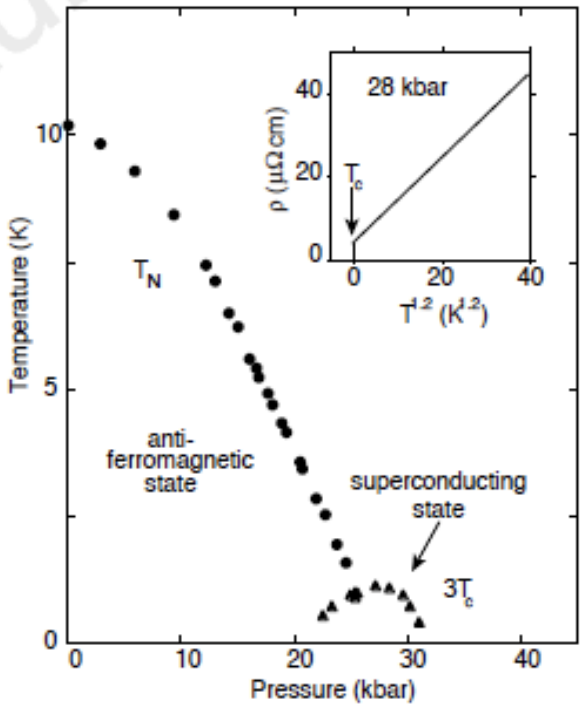

Figure 2 Temperature–pressure phase diagram of high-purity single-crystal $CePd_2Si_2$. Superconductivity appears below T_c in a narrow window where the Néel temperature T_N tends to absolute zero. Inset: the normal state *a*-axis resistivity above the superconducting transition varies as $T^{1.2\pm0.1}$ over nearly two decades in temperature[27,30]. The upper critical field B_{c2} at the maximum value of T_c varies near T_c at a rate of approximately –6 T/K. For clarity, the values of T_c have been scaled by a factor of three, and the origin of the inset has been set at 5 K below absolute zero.

Mathur et al. Nature **394**, 39 (1998)

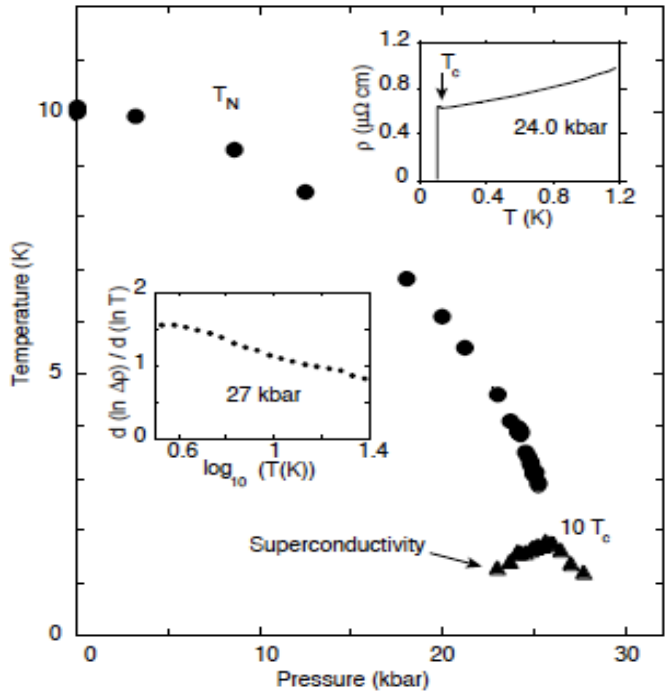

Figure 3 Temperature–pressure phase diagram of high-purity single-crystal $CeIn_3$. A sharp drop in the resistivity consistent with the onset of superconductivity below T_c is observed in a narrow window near p_c, the pressure at which the Néel temperature T_N tends to absolute zero. Upper inset: this transition is complete even below p_c itself. Lower inset: just above p_c, where there is no Néel transition, a plot of the temperature dependence of $d(\ln \Delta\rho)/d(\ln T)$ is best able to demonstrate that the normal state resistivity varies as $T^{1.6\pm0.2}$ below several degrees K (ref. 29) ($\Delta\rho$ is the difference between the normal state resistivity and its residual value—which is calculated by extrapolating the normal-state resistivity to absolute zero). For clarity, the values of T_c have been scaled by a factor of ten. The resistivity exponents of $CeIn_3$ and $CePd_2Si_2$ may be understood by taking into account the underlying symmetries of the antiferromagnetic states and using the magnetic interactions model. Superconductivity near n_c in pure samples is expected to be a natural consequence of the same model.

Crystal Structures

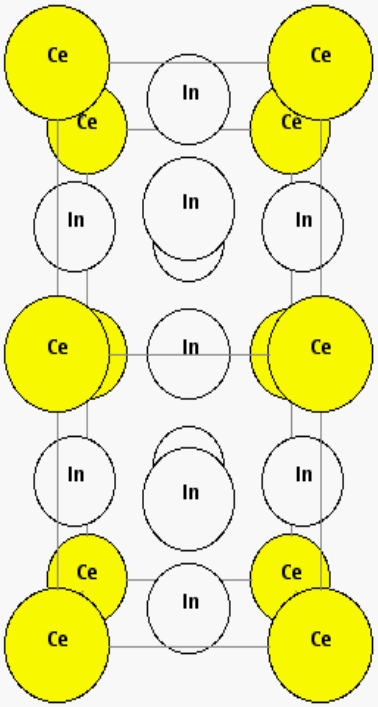

$CeIn_3$

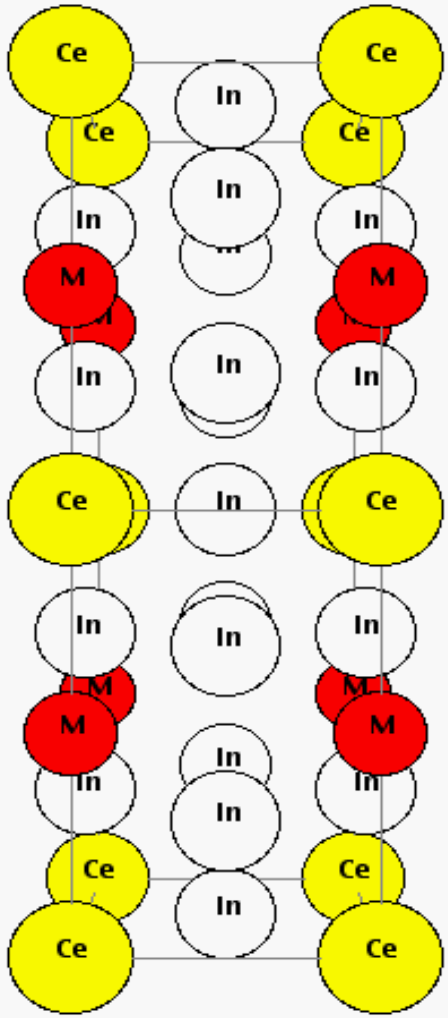

$CeMIn_5$

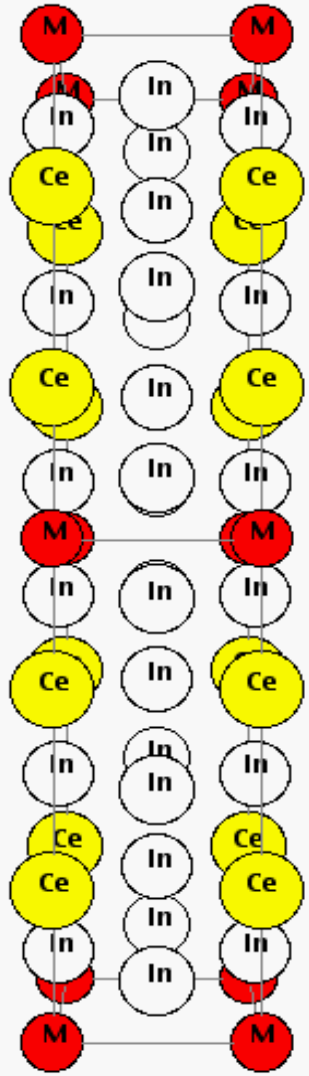

Ce_2MIn_8

M = Co, Rh, Ir (isovalent)

AF and Superconductivity in $CeMIn_5$ systems

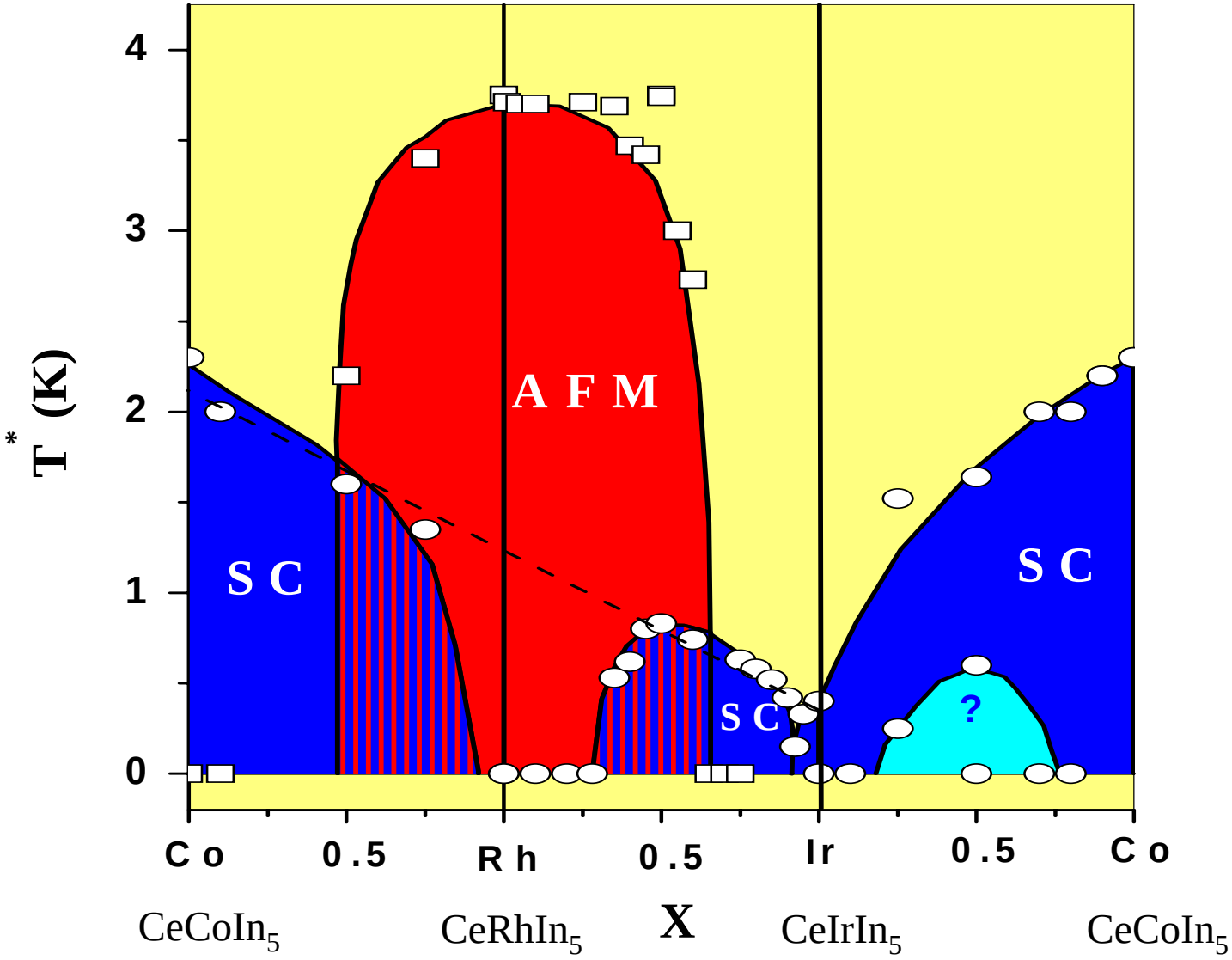

P. Pagliuso *et al.*, PRB **64**, 100503 (2001).

Phase diagram of $CeRhIn_5$ (Park and Thompson)

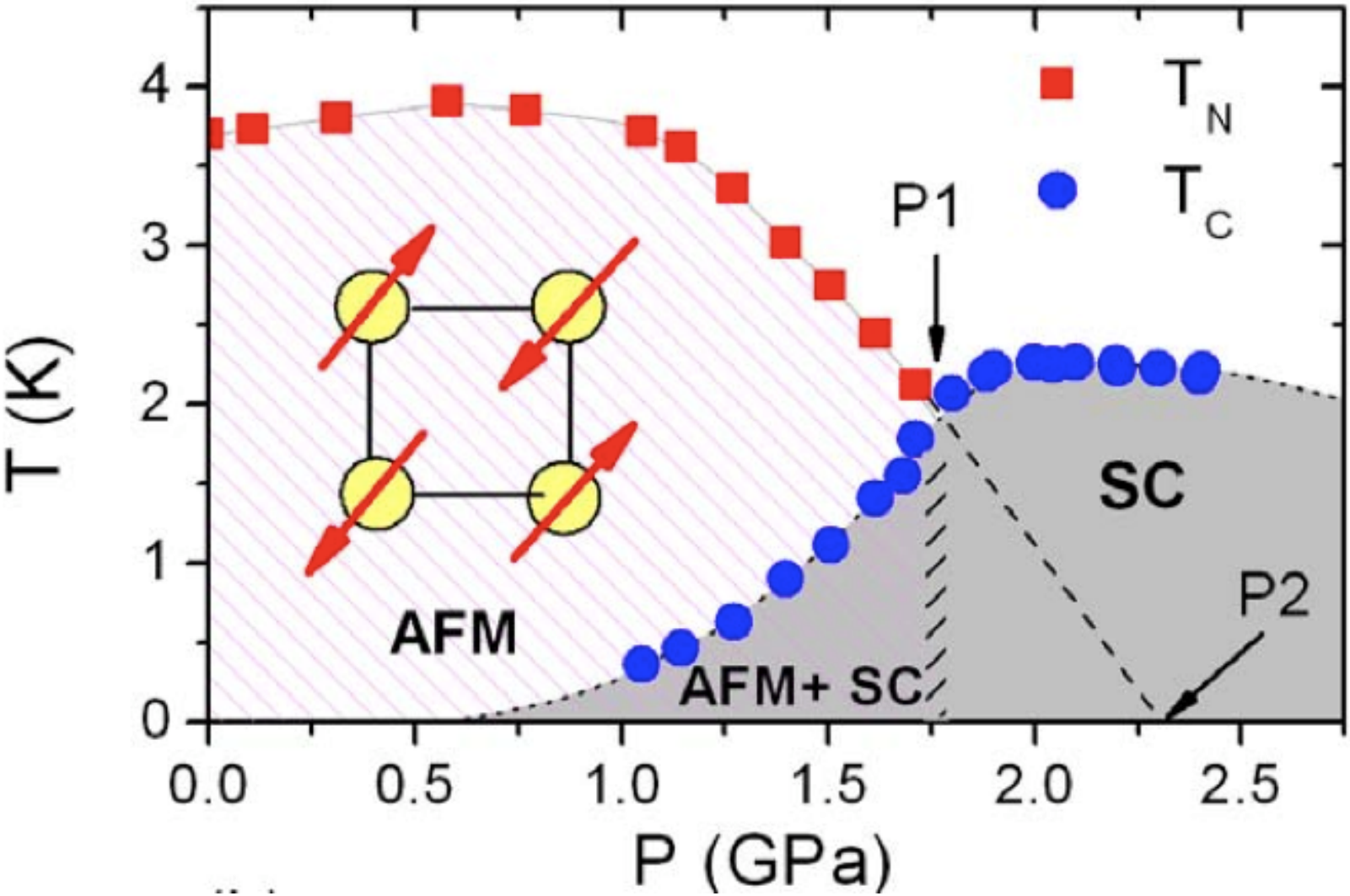

Onuki et al. J. Alloys Cpds. **408-412**, 27 (2006)

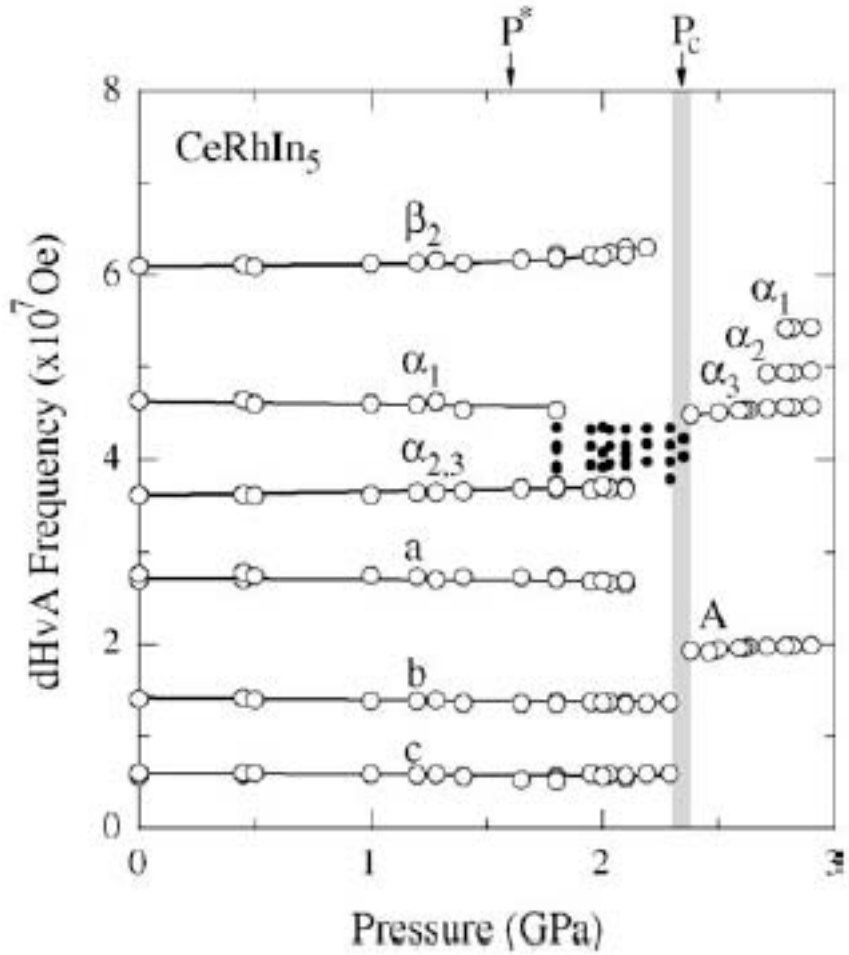

Fig. 6. Pressure dependence of the dHvA frequency in $CeRhIn_5$.

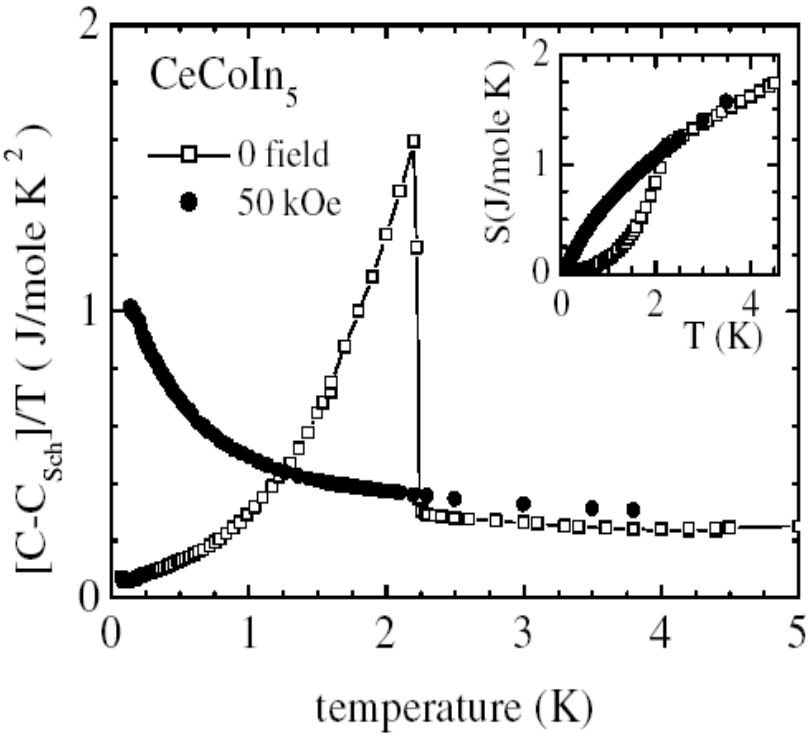

Figure 2. Specific heat divided by temperature versus temperature for $CeCoIn_5$. For both the zero-field (open squares) and 50 kOe (solid circles) data, a nuclear Schottky contribution, due to the large nuclear quadrupole moment of In, has been subtracted. The inset shows the entropy recovered as a function of temperature in the superconducting (open squares) and field-induced normal (solid circles) states.

Stock et al. Phys. Rev. Lett. **100**, 087001 (2008)

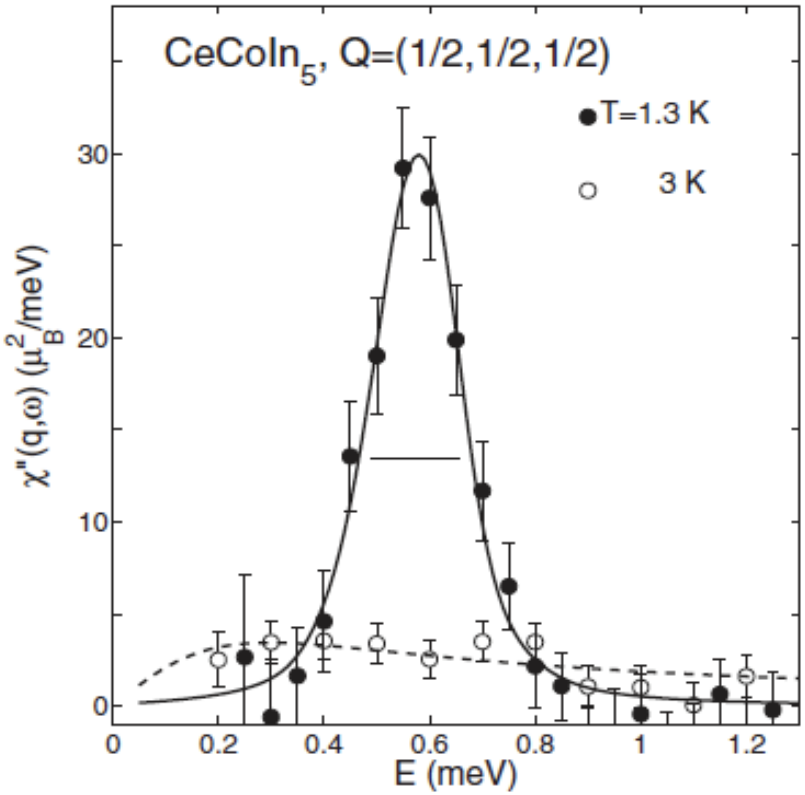

FIG. 1. The imaginary part of the dynamic susceptibility at $\mathbf{Q} = (\frac{1}{2}\,\frac{1}{2}\,\frac{1}{2})$ is plotted in the normal (3 K) and in the superconducting (1.35 K) states. A background taken at $\mathbf{Q} = (0.3, 0.3, 0.5)$ and $\mathbf{Q} = (0.7, 0.7, 0.5)$ was subtracted. The horizontal bar is the resolution width.

Stock et al. Phys. Rev. lett. **100**, 087001 (2008)

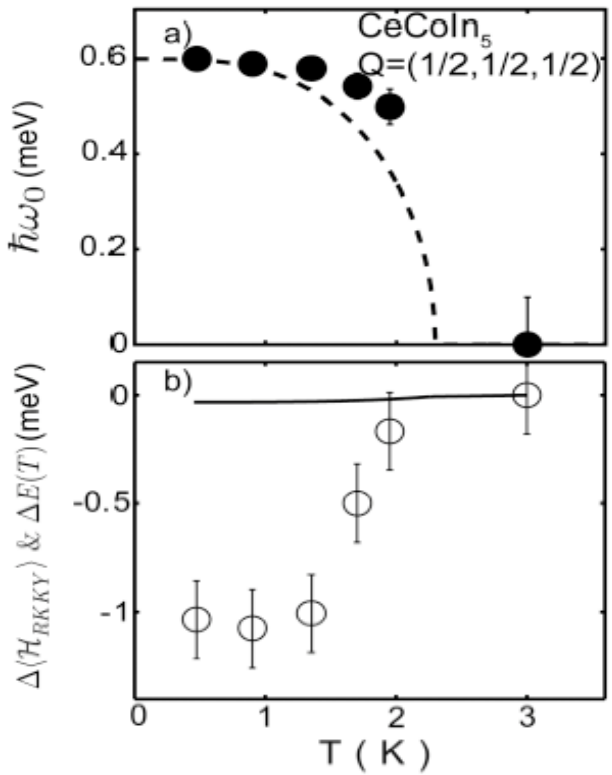

FIG. 4. (a) Spin resonance energy versus T compared to the scaled d-wave BCS superconducting gap amplitude described text. (b) thermal variation for $T < 3$ K of the exchange energy, $\Delta\langle\mathcal{H}_{\rm RKKY}\rangle$, derived from inelastic neutron scattering compared to the overall electronic energy derived from specific heat data: $\Delta E(T) = \int_0^T C(T')dT' - \int_0^{3\rm K} C(T')dT'$. Note there is an overall 50% systematic error bar on the normalization of the data for $\Delta\langle\mathcal{H}_{\rm RKKY}\rangle$ in (b).

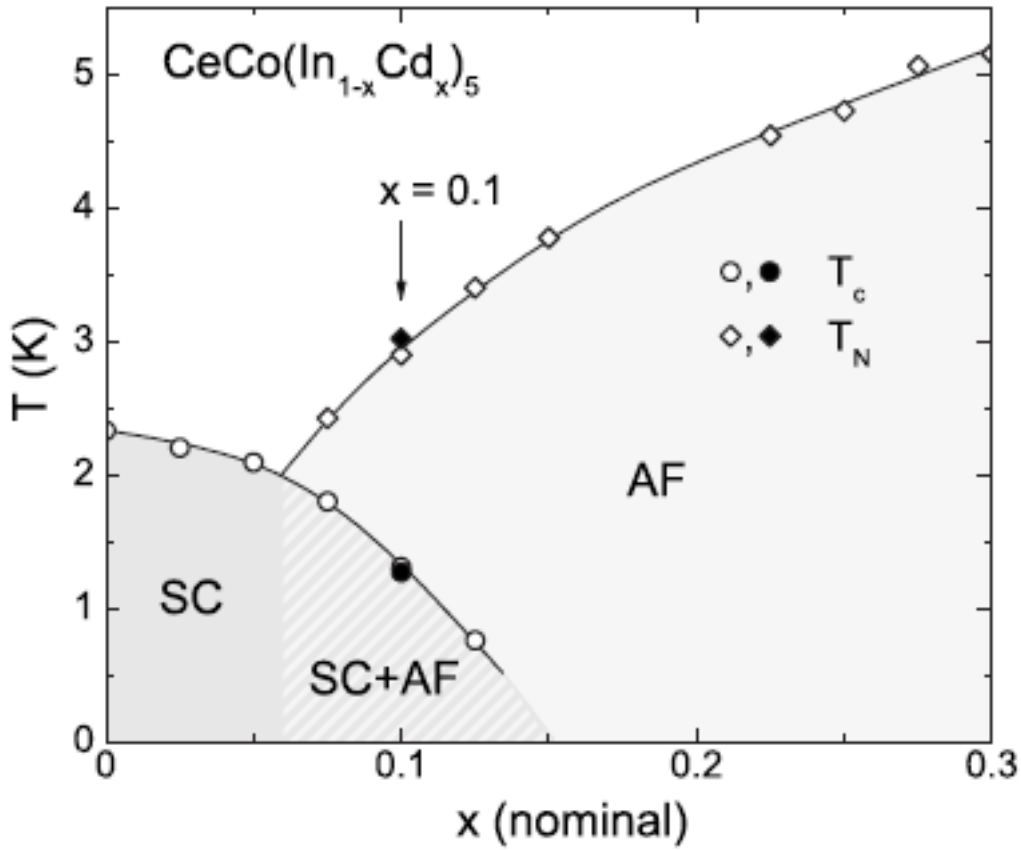
CeCo(In1-xCdx)5
x = 0.1
Tc
TN
AF
SC
SC+AF
T (K)
x (nominal)
0
1
2
3
4
5
0
0.1
0.2
0.3

M. Nicholas et al. Phys. Rev. B **76**, 052401 (2007)

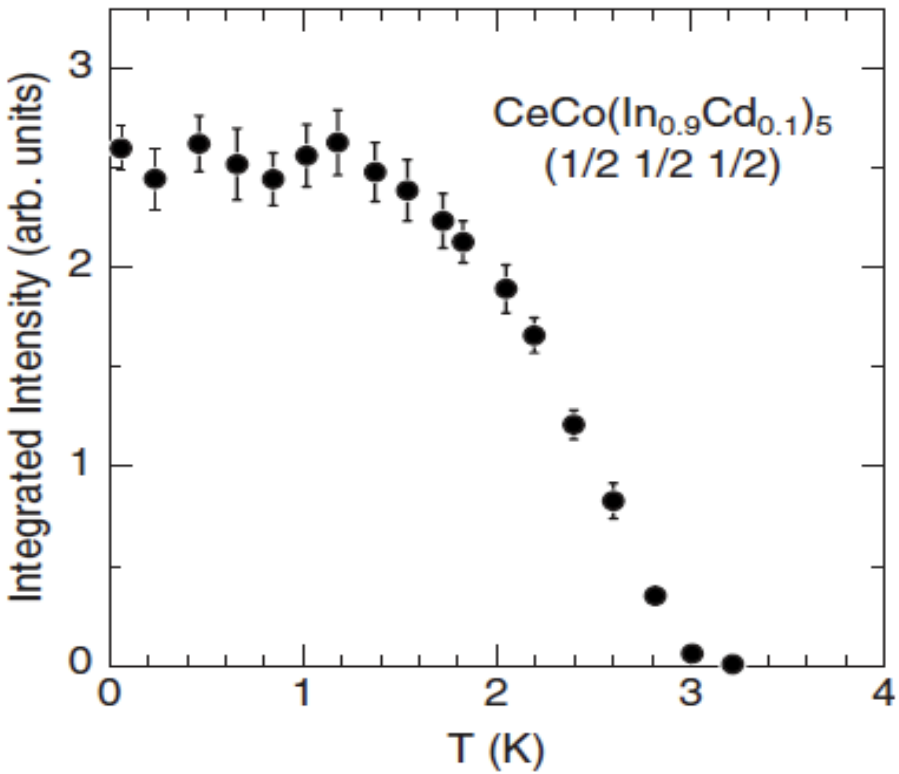

FIG. 4. Temperature dependence of the integrated magnetic intensity as obtained by Gaussian fits to the scans across $Q = \left(\frac{1}{2}, \frac{1}{2}, \frac{1}{2}\right)$.

generic cuprate phase diagram

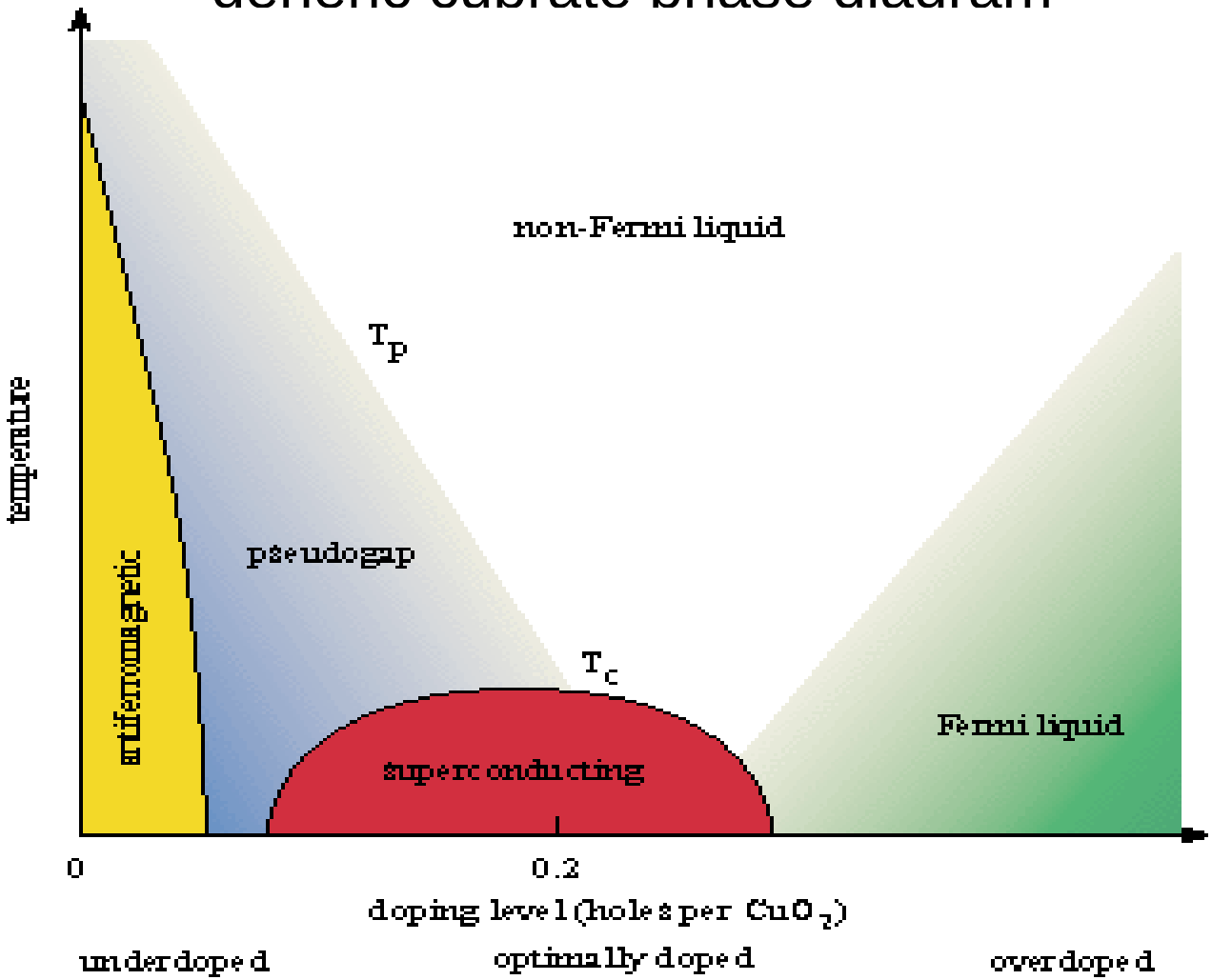

Doiron-Leyraud et al. arXiv: 0912.2049

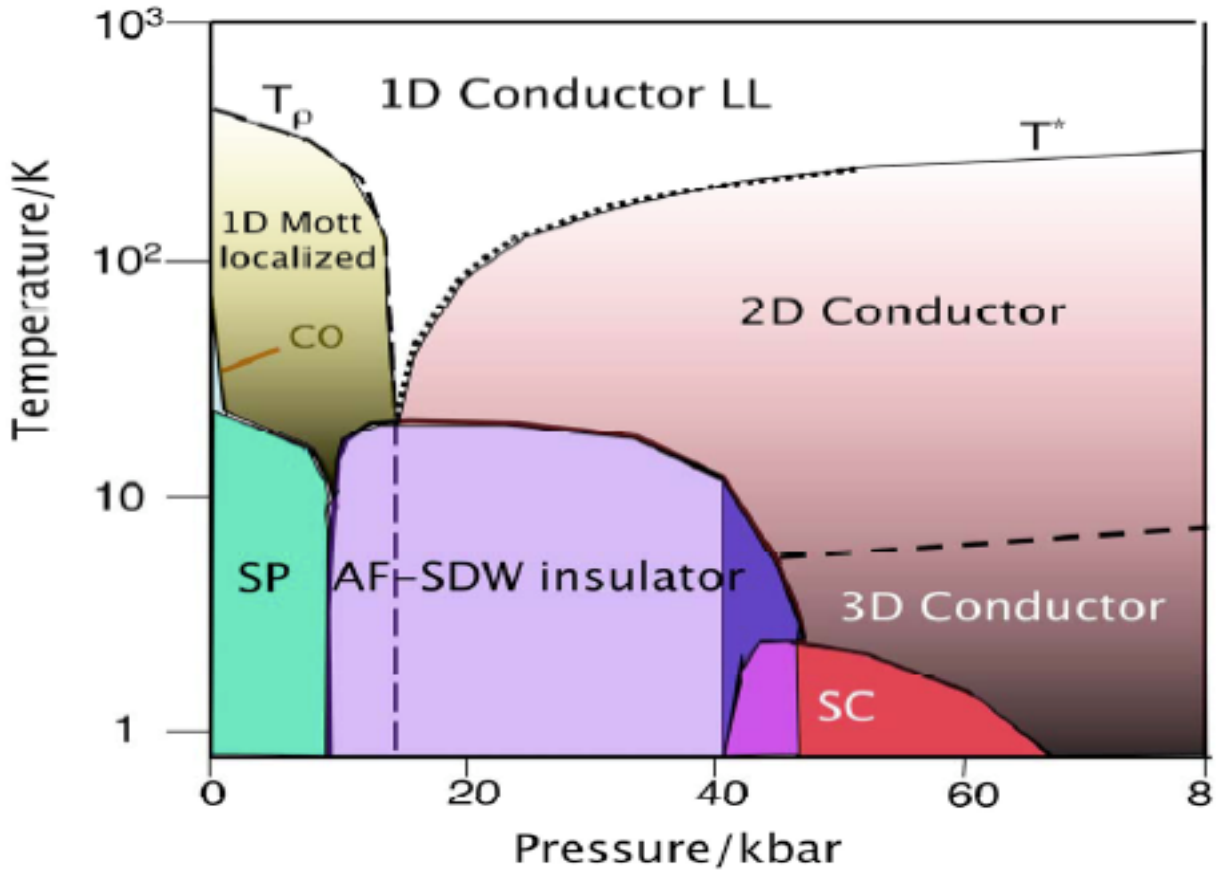

Figure 1: Generic temperature-pressure phase diagram of the $(TM)_2X$ family of organic conductors. The diagram is drawn for the compound $(TMTTF)_2PF_6$ taken for the origin of the pressure scale. The location of the compounds $(TMTSF)_2PF_6$ and $(TMTSF)_2ClO_4$ under ambient pressure are $\approx$ 37 and 47 kbar respectively in this diagram.

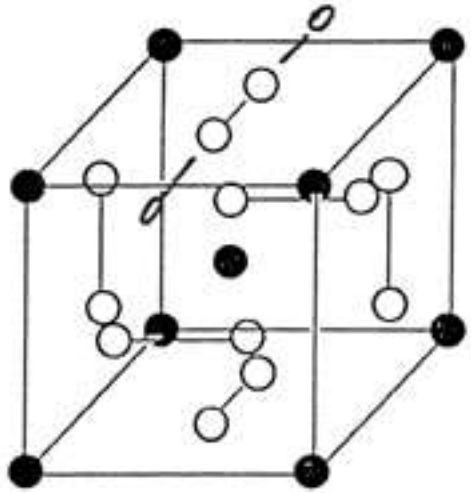

FIGURE 9–7. The V_6Si_2 cubic building block for V_3Si and related A-15 supercor Shaded circles in the center and at each of the eight vertices correspond to silico whereas the pairs of open circles (each linked by a straight line) in each of the correspond to vanadium atoms.

reference cube (Figure 9–7), namely one in each face. The V–V bonc vanadium chains, although equivalent in the overall structure, are following two types relative to a V_6Si_2 reference cube with which associated:

1. The first type (A) consists of bonds between two vanadium atc given face of the V_6Si_2 reference cube. Such V–V bonds are sha between the two cubes sharing the face containing the vanadium
2. The second type (B) consists of bonds between a vanadium atom adjacent vanadium atom in the chain *not* associated with th reference cube. Such V–V bonds are shared between four adjace cubes.

Batterman and Barrett Phys. Rev. **145**, 296 (1966)

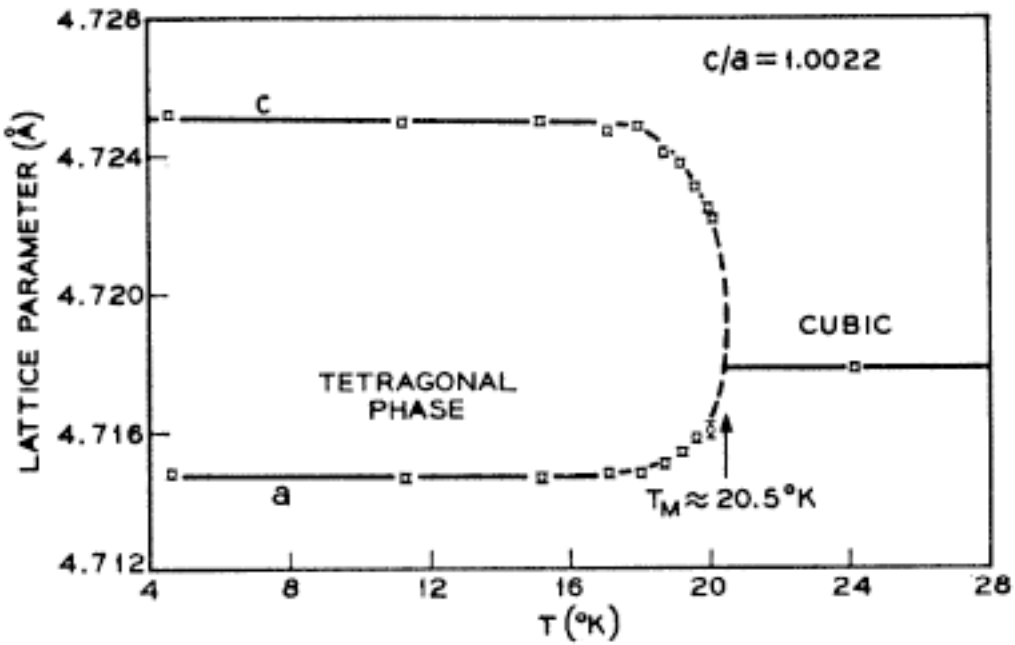

FIG. 6. c and a parameter versus T of a well-behaved specimen. The data in the dashed region were difficult to obtain because of peak overlap and broadening. All evidence indicates that the change is smooth but rapid in this region.

Schilling V_3Si: $T_{Martensitic}$ / T_c

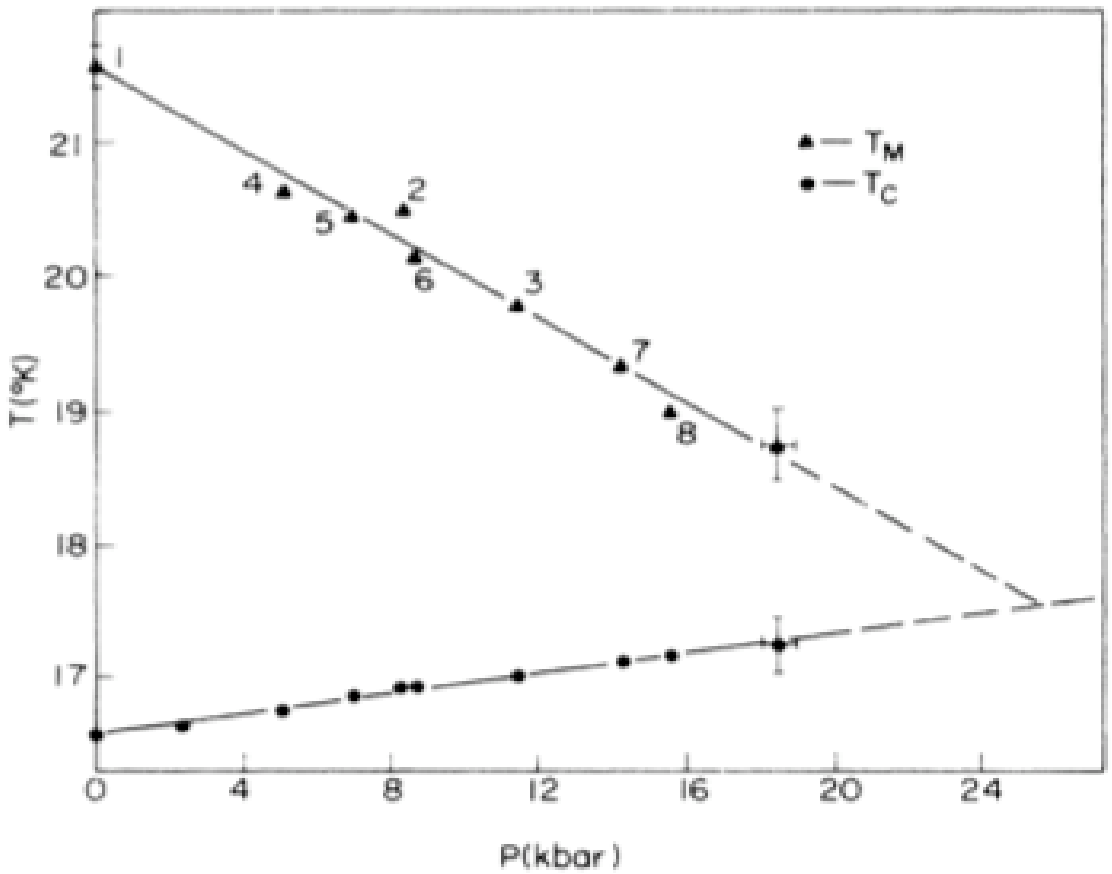

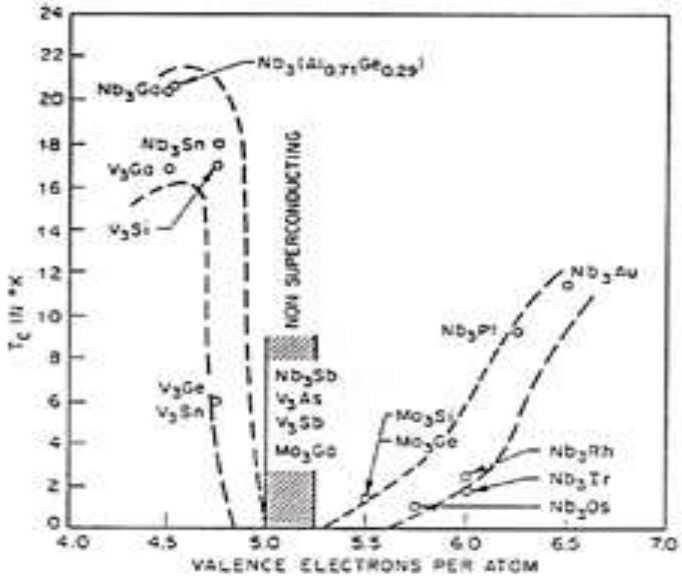

Fig. 24. Superconducting critical temperature versus the number of valence electrons per atom for some A_3B Cr_3Si (A15) compounds.

where $\langle h\omega \rangle_{av}$ is the average energy of the phonons that scatter electrons at the Fermi surface; $N(0)$ is the normal-state density of electron states per unit energy range at the Fermi surface, and V is an interaction energy of electrons close to the Fermi surface, and is composed of an attractive electron–electron pairing potential arising from the electron–phonon interaction and a Coulomb repulsive interaction between electrons. Here k is Boltzmann's constant. The above equation is also written in terms of the Debye temperature θ_D by taking $1.14\langle h\omega \rangle_{av}$ proportional to $k\theta_D$:

$$T_c = 0.85\theta_D \exp[-1/N(0)V]$$

The term $N(0)$ can be computed from a knowledge of the coefficient of electronic contribution γ to the heat capacity, determined from low-temperature heat capacity measurements. The Debye temperature θ_D can also be determined from heat capacity data as

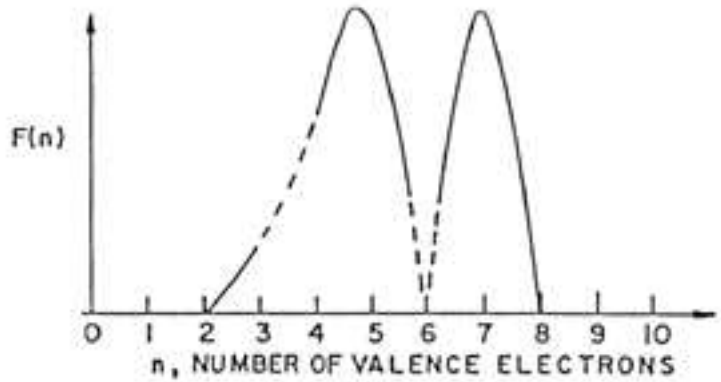

3. Matthias' empirical relation for the superconducting transition temperature of TM alloys. $F(n)$ $(n \equiv z)$ measures the transition temperature T_c (*17*).

he above makes it reasonable to think in terms of a universal model for conduction bands of the TM. One imagines a "rigid band" structure for e metals into which electrons are "poured," with the properties of a given al depending on its number of conduction electrons per atom Z. When ı a simple picture breaks down, we will return to question its validity. In remainder of this section, we develop only the main considerations involved uch a model (more complete discussions are indicated for the interested ler).

one could gradually move the atoms (assumed initially to be infinitely ırated) of a given element together, one would find, after perhaps a well-ned transition (*18–21*), that the outer atomic *s*-electron wave functions ıld "join," forming a band of (itinerant) electrons. The band would have

Highest T_c found in proximity to competing “localized” phase

- holds for BCS, heavy Fermions, organics, cuprates and pnictides
- the competing phase, afm in heavy Fermions, terminates where it intersects the $T_c$boundary and does not extend into the superconducting phase
- localized: in BCS, lattice distorted; in heavy Fermions, local moment magnetism; in cuprates, the psuedo-gap phase.
- electronics highly non-adiabatic
- superconductivity runs in structures
- superconductivity is where physics becomes chemistry